How and to what extent do carbon materials catalyze solar hydrogen production from water?

Young Kwang Kim[a], Hyunwoong Park[b],*

[a] Department of Physics, Kyungpook National University, Daegu 702-701, Republic of Korea
[b] School of Energy Engineering, Kyungpook National University, Daegu 702-701, Republic of Korea

A B S T R A C T

The aim of this study is to find key physicochemical properties of carbon materials in catalyzing the photocatalytic H_2 production from visible light-irradiated aqueous suspensions of carbon/CdSe composites. For this, we have employed five different carbon materials (activated carbons, carbon fibers, multi- and single-walled nanotubes, and graphites) without and with acid treatment, and two carbon materials obtained from graphite (graphite oxides and reduced graphene oxides). Detailed surface analyses for the bare carbon materials and carbon/CdSe composites were completed to characterize their physicochemical properties. Most virgin (non-treated) carbon materials are beneficial in catalyzing the photocatalytic H_2 production of carbon/CdSe composites, and such catalytic effects are significantly enhanced by their acid treatment by a factor of 3–7. Systematic investigation indicates that the surface area, the degree of disordered carbon (i.e., I_D/I_G ratios), and the electrical conductivity (σ) of carbon materials display the correlations with H_2 production of carbon/CdSe composites. However, the first two factors could not explain well the enhanced H_2 production by acid treatment of carbon materials, whereas the last factor exhibits the linearity with the H_2 amounts even for the acid-treated carbon materials. High electrical conductivity appears to facilitate the photogenerated electron transfer from CdSe to neighboring carbon materials, leading to inhibition of charge pair recombination as evidenced by photoluminescence study.

© 2012 Elsevier B.V. All rights reserved.
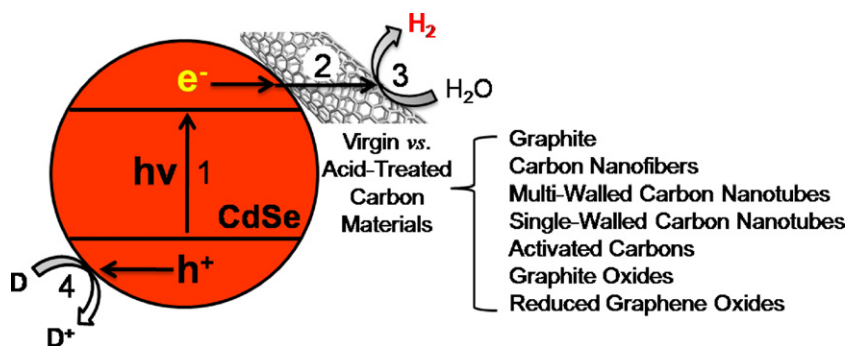
1. Introduction

Semiconductor-based solar hydrogen is a promising and renewable energy carrier with a great application potential to meet the future global energy demands [1–3]. In order for solar hydrogen systems to be effective and efficient, semiconductors must absorb a wide range of solar spectrum, create many electron–hole pairs per incident photons, and have rapid charge separation and efficient interfacial charge transfer process. Among these conditions, the last could be achieved simply by coupling the semiconductors to hydrogen evolving catalysts such as traditional platinum group metals (PGMs: Pt, Pd, Ru, etc.) [4]. Yet the high cost of PGMs substantially increases the cost of solar hydrogen and hinders the practical application of semiconductor systems.

Recently, carbon materials of relatively low cost [5] have been reported as an alternative to PGMs in photoelectrochemistry [6–8] and photocatalysis [9–13]. They are diverse from carbon blacks, activated carbons (AC) [14], carbon nanofibers (CNF) [15,16], single- and multi-walled carbon nanotubes (SWNT [10,17–19] and MWNT [11,18,20], respectively), graphites (GP)

[21–23], graphite oxides (GO) [24,25], and reduced graphene oxides (RGO) [9,12,13,26–30]. These carbon materials are very attractive in terms of different physicochemical properties in thermal conductivity, electrical resistivity, BET surface area, as well as *sp* valence hybrid configuration [5]. The primary reason for the coupling of semiconductors (e.g., TiO_2 [9,17,18,20,24,26–33], $BiVO_4$ [7], CdS [10–13,19,20], and CdSe [20]) with carbon materials appears to be the unique physicochemical properties of carbon materials, such as low electrical resistivity, which thereby enhances the interfacial charge transfers. Indeed, the electrical resistivity of graphite is as low as $0.4 \times 10^{-6}\ \Omega\,m$ (parallel to basal plane), whereas those of pyrolytic carbons and carbon fibers increase by over 10 times [5]. Because of this property, the photoconversion performances of semiconductors were improved when combined with SWNT [10,17–19,31], MWNT [11,20], and RGO [7,9,12,13,24,26–30,34]. Large surface area also may be one of the primary reason for the wide use of the carbon materials (e.g., activated carbon with BET surface area of ~1000 m^2/g) because it increases the adsorption of substrates on the semiconductor surface and facilitates the photocatalytic reactions [5,35]. Nevertheless, we note that even though a number of papers have appeared regarding the application of diverse carbon materials in photovoltaics, photoelectrochemistry, and photocatalysis, no systematic comparison of carbon materials for their effects on photoconversion have been reported yet.

* Corresponding author. Tel.: +82 53 950 8973.
  E-mail address: hwp@knu.ac.kr (H. Park).

Scheme 1. Schematic illustration for photocatalytic H_2 production in visible-light irradiated aqueous suspensions of carbon/CdSe composites with various carbon materials without and with acid treatment. Overall reaction proceeds via (1) light absorption, (2) interfacial transfer of photogenerated electrons at carbon/CdSe and subsequent electron transport on carbon materials, (3) hydrogen production on the surface of carbon materials, and (4) hole transfer to electron acceptors.

The aim of this study is to address the following questions: (1) Which physicochemical property of carbon materials is the primary factor catalyzing solar hydrogen in water? (2) Why do carbon materials have different catalytic effects? (3) To what extent can the carbon materials enhance solar hydrogen production? For this aim, we have employed five different commercially available carbon materials (activated carbons, carbon fibers, multi-walled nanotubes, single-walled nanotubes, and graphites) and two carbon materials converted from the commercial graphite (graphite oxides and reduced graphene oxides). For solar hydrogen, CdSe as a model semiconductor was synthesized on these carbon materials. The carbon materials were tested without and with acid treatment because the surface treatment was expected to change the physiochemical properties of the carbon materials, which in turn may affect the solar hydrogen efficiency as well (Scheme 1). Several experimental data (BET surface area, UV–vis absorption, XPS, Raman analysis, electrical conductivity, SEM, Cd ion adsorption, photoluminescence, etc.) were obtained. On the basis of the data, we explored to find possible key factors affecting the overall solar hydrogen efficiencies.

2. Experimental

2.1. Materials

2.1.1. Carbon materials

Graphite (<20 μm, Sigma), multi-walled carbon nanotubes (CM-100, Hanwha Nanotech), single-walled carbon nanotubes (ASA-100F, Hanwha Nanotech), carbon nanofibers (CNF-LSA, Carbon Nano Material Technology), and activated carbons (Alfa Aesar) were used as-received or after acid treatment. Graphite oxides and reduced graphene oxides were prepared by following a modified Hummer's method (see Supporting Information) [36]. For acid-treated carbon (a-carbon) materials, as-received carbon materials were suspended and stirred in a mixed aqueous solution of 1 M HNO_3 and 1 M HCl for 30 min. Then, they were filtered with 0.45-μm PTFE filters (Millipore), washed with distilled water, and dried overnight at 80 °C.

2.1.2. CdSe and carbon/CdSe samples

The preparation method of CdSe was found elsewhere [37]. In brief, metallic selenium (Se, Daejung) and sodium sulfite (Na_2SO_3, Daejung) powders were dissolved at 20 mM in de-ionized water (0.05 L) and mixed over 1 h at 70 °C in a round-bottom flask that was immersed in an oil bath. This reaction produces $SeSO_3^{2-}$ of 1 mmol. An aqueous solution (0.05 L) of cadmium acetate (20 mM, Daejung) was slowly dropped into the $SeSO_3^{2-}$ solution and mixed for 6 h. Then, the mixed solution was filtered with a 0.45-μm filter, washed with distilled water, and dried overnight at 80 °C after collection.

For carbon/CdSe and a-carbon/CdSe samples, each carbon material (or a-carbon material) of 60 mg was suspended in the cadmium acetate solution for 6 h, and the suspension was dropped to the $SeSO_3^{2-}$ solution. Then, the resultant particles were collected and dried overnight at 80 °C.

2.2. Photocatalytic H_2 production

As-prepared composites were suspended at 1 g/L in an aqueous solution of 0.1 M Na_2S and 0.1 M Na_2SO_3 as a mixed electron donor in a Pyrex-glass reactor equipped with a quartz disc for light penetration. The volumes of reaction suspension and headspace were 25 mL and 14 mL, respectively. The pH of suspension was about 11.5 in the presence of the electron donor, and no further pH change was made. Prior to irradiation, N_2 (>99.9%) gas was purged through the suspension for 30 min to remove dissolved oxygen in the aqueous phase as well as in the headspace. Visible light (λ > 420 nm) was irradiated to the reactor by inserting a long-wave pass filter between the reactor and a solar simulator equipped with AM 1.5 G filter (LS-150 Xe, Abet Technologies). The amounts of H_2 produced were quantified using a gas chromatograph device (ACME 6100, Younglin Instrument) equipped with a thermal conductivity detector.

2.3. Surface analysis methods

Thermal gravimetric analysis was carried out at a scan rate of 10 °C/min in the range from room temperature to 1000 °C with simultaneous air-purging (Seiko, TG/DTA 320). Specific surface areas were determined on a surface analyzer (Quantachrome Nova 200 Autosorb 1-C) with flowing degassing gas (He) at 200 °C for 2 h. Operational relative pressure (P/P_0) range was 0.083–0.985. Scanning electron microscopy (SEM) measurements were performed by a field emission electron microscope (Hitachi S-4800) at an operation voltage of 3 kV. For Raman analyses, round plate samples (radius 0.5 cm) were prepared using a typical pelletizer. The employed Raman spectrometer (Almega X, Thermo) consisted of a confocal microscope, a single spectrograph fitted with holographic notch filters for spectroscopy mode, and a multichannel air cooled CCD detector. The excitation wavelength was the 780 nm-line of Nd:YAG laser (5000 mW). Electrical conductivities were obtained with a four-point probe (CMT-SR3000, AIT corp.). Sample pellets were prepared and their electrical conductivities were estimated from the measured values of resistivity. In order to examine the exciton recombination rate, photoluminescence (PL) spectra were obtained with a PL spectrometer (Acton Research Co., Spectrograph 500i) equipped with an intensified photo diode array detector (Princeton Instrument Co., IRY1024, USA). The PL light source was a He–Cd laser (Kimon, 1K, Japan) with a wavelength of 325 nm and
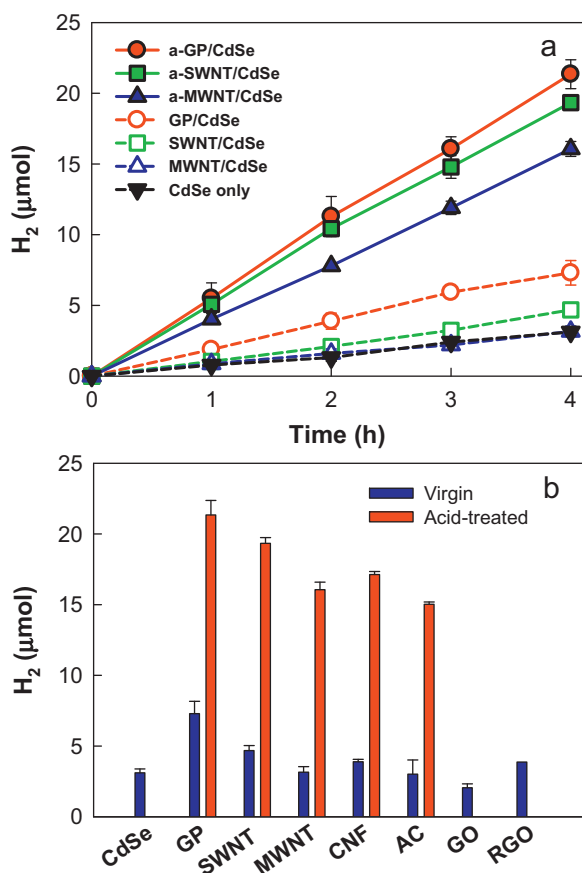
Fig. 1. (a) Time profiled H_2 productions and (b) comparison of H_2 amounts (produced after 4 h) in visible light-irradiated carbon/CdSe composite suspensions. GP: graphite; SWNT: single-walled carbon nanotubes; MWNT: multi-walled carbon nanotubes; CNF: carbon nanofibers; AC: activated carbons; GO: graphite oxides; RGO: reduced graphene oxides. a-Carbon materials refer to acid-treated ones. [Composite catalyst] = 0.5 g/L; $[Na_2S]_0 = [Na_2SO_3]_0 = 0.1$ M; N_2 purged through suspensions for 30 min prior to irradiation ($\lambda > 420$ nm).

a power of 50 mW. For quantifying adsorbed cadmium ions (Cd^{2+}) in carbon materials, the amounts of cadmium before and after filtration through 0.45-μm PTFE filters (Millipore) were estimated using an inductively coupled plasma atomic emission spectrometer (Optima 7300DV, PerkinElmer) with RF frequency of 40 MHz and wavelength range from 165 to 782 nm was employed. The surface elemental composition of samples was determined by X-ray photoelectron spectroscopy (XPS, Kratos, XSAM 800 pci) using the Mg Kα line (1253.6 eV) as the excitation source. The binding energies of all peaks were referenced against the Au 4f line originating from the gold powder mixed with the samples. The optical absorption spectra of samples were obtained with a UV–vis spectrophotometer (Shimadzu UVPC-2401) equipped with a diffuse-reflectance attachment (Shimadzu IRS-2200). All sample powders were mixed with $BaSO_4$ (1:1 by weight), and their absorption spectra were measured against $BaSO_4$.

3. Results and discussion

3.1. Photocatalytic activities and surface characterization of carbon/CdSe samples

Fig. 1 compares photocatalytic hydrogen production in visible light ($\lambda > 420$ nm)-irradiated suspensions of carbon/CdSe in the presence of electron donors (0.1 M Na_2S and 0.1 M Na_2SO_3). The samples were prepared by simple hydrolysis of Cd(II) ions and Se(II)

ions with 1:1 stoichiometry. No post-annealing was applied so as to avoid any possible physicochemical change of carbon materials, although all the carbons exhibited thermal stability up to ca. 300 °C (Fig. S1 in Supporting Material). Irradiation to bare CdSe produced H_2 linearly at a rate of ca. 0.75 μmol h^{-1}, yet CdSe with virgin (non-treated) and acid-treated graphite particles (GP and a-GP, respectively) enhanced the H_2 production rate by a factor of approximately 2.5 and 7, respectively. Such enhancements by GP and a-GP were similarly found in the other carbon samples (Table 1). It should be pointed that when virgin carbon materials were used, the amount of H_2 was greatest with GP followed by SWNT, the tendency of which was quite similar to that of acid-treated carbon materials. In the cases of GO and RGO, no acid treatment was applied to them because they were already obtained from GP via a chemical oxidation (and reduction for RGO). Hence an additional treatment with acid may transform their physicochemical structures into unwanted structures. GO and RGO exhibited low catalytic activities for hydrogen production, which are quite different from the findings of previous studies [12,13] employing CdS and RGO likely due to different experimental conditions (the kind and surface state of semiconductor, ratios between semiconductor and RGO, electron donors, etc.).

In order to study in detail the effect of various types of carbon material and surface treatment, the surfaces of carbon/CdSe composites without and with the acid treatment of carbon materials were analyzed. Fig. 2 shows the SEM images of six different composites. It is apparent that CdSe was formed well on the surface of carbon materials despite the existence of particle aggregation. It should be noted that the SEM images were obtained from dried samples and hence could not represent the real morphology in an aqueous environment. Also, the aggregation of semiconductor particles often causes light-scattering (negative effect), whereas in many cases it reduces the charge pair recombination (positive effect) [38,39]. In the latter, the charge pairs created in a single semiconductor particle are effectively transferred to neighboring semiconductor particles (vectorial charge transfer) [38–40].

An XPS study was also completed for CdSe composites with virgin and acid-treated graphite particles (Fig. 3). It is obvious that the binding energy and the shape of O 1s band for bare graphite were different from those for GP/CdSe, suggesting the interaction between oxygen atoms of graphite and CdSe (or its precursors). The resolution of the GP O 1s band indicated that there were various oxygen atoms as follows: (Fig. 3a): N–O (536.2 eV), C–O (533 eV), C=O (531.5 eV), CO_3^{2-} (535.1 eV), COOH (530.5 eV), and H–O (527.8 eV) [41]. Acid-treated graphite also had a similar set of oxygen atoms (Fig. 3b). When CdSe was loaded on GP and a-GP, the O 1s bands shifted to lower energy direction, resulting from the existence of the oxygen atoms coordinated primarily to Cd^{2+}, such as $CdCO_3$ (531.2 eV), $Cd(OH)_2$ (530.7 eV), and CdO (529.2 eV) (Fig. 3c and d) [41–43]. The elemental amounts of CO_3^{2-} in GP and a-GP were similar with approximately 4%, but those of $CdCO_3$ in GP/CdSe and a-GP/CdSe ranged between 35% and 54%, accompanying the decrease of percentage of C–O band from ~60% to ~30%. Therefore, the spectral changes of O 1s band by loading of CdSe resulted mostly likely from the formation of $CdCO_3$ and decrease of C–O bonding irrespective of graphite kind. It is of note that the binding energies of Cd 3d and Se 3d with a-GP were found to shift by 0.245 and 0.125 eV to lower and higher energy directions, respectively, as compared to GP (Fig. 3e and f). Such shifts suggest that Cd^{2+} may exist as a more reduced state, whereas Se^{2-} does as a more oxidized state on a-GP surface. Therefore, acid treatment of graphite (as well as other carbon materials) appears to provide a different environment for CdSe formation by catalyzing partial redox reaction of cadmium and selenide, which resulted most likely in the aggregation of CdSe particles on the acid-treated carbon materials.

Table 1
Comparison of carbon materials for their physicochemical properties, adsorption capacities for Cd^{2+}, and photocatalytic hydrogen productions on carbon/CdSe composite.

Samples		Surface area (m^2/g)	Electrical conductivity (S/m)	I_D/I_G[b]	$[Cd^{2+}]_{ads}$ (mmol/g)[c]	$[H_2]$ (μmol)[d]
AC	Virgin	851	1.70×10^{-1}	1.56	13.6	3.01($\pm$1.00)
	Treated[a]	950	1.19×10^4	1.76	14.0	17.0($\pm$0.1)
CNF	Virgin	130	2.87×10^1	1.39	12.7	3.90($\pm$0.17)
	Treated	140	1.89×10^4	2.07	12.9	17.1($\pm$0.2)
MWNT	Virgin	22	1.87×10^3	1.50	12.4	3.16($\pm$0.27)
	Treated	178	1.42×10^5	1.79	13.5	16.1($\pm$0.5)
SWNT	Virgin	100	2.93×10^2	0.04	13.2	4.68($\pm$0.36)
	Treated	134	4.30×10^4	0.31	12.3	19.5($\pm$0.4)
GP	Virgin	14	1.81×10^4	0.84	12.3	7.30($\pm$0.87)
	Treated	9	1.46×10^6	1.04	12.6	21.4($\pm$1.0)
GO	–	–	1.65×10^0	1.35	13.1	2.06($\pm$0.28)
RGO	–	23	1.01×10^3	1.31	12.7	3.87($\pm$0.35)

[a] Carbon samples were suspended in an aqueous mixture of 1 M HNO_3 and 1 M HCl for 30 min and recovered after washing with distilled water and drying at 80 °C.
[b] Raman intensity ratios between D band and G band.
[c] $[Cd(II)]_{initial}$ = 10 mM (0.1 L); [carbon] = 0.06 g.
[d] Produced in 4 h under visible light (λ > 420 nm) in the presence of 0.1 M Na_2SO_3 and 0.1 M Na_2S.
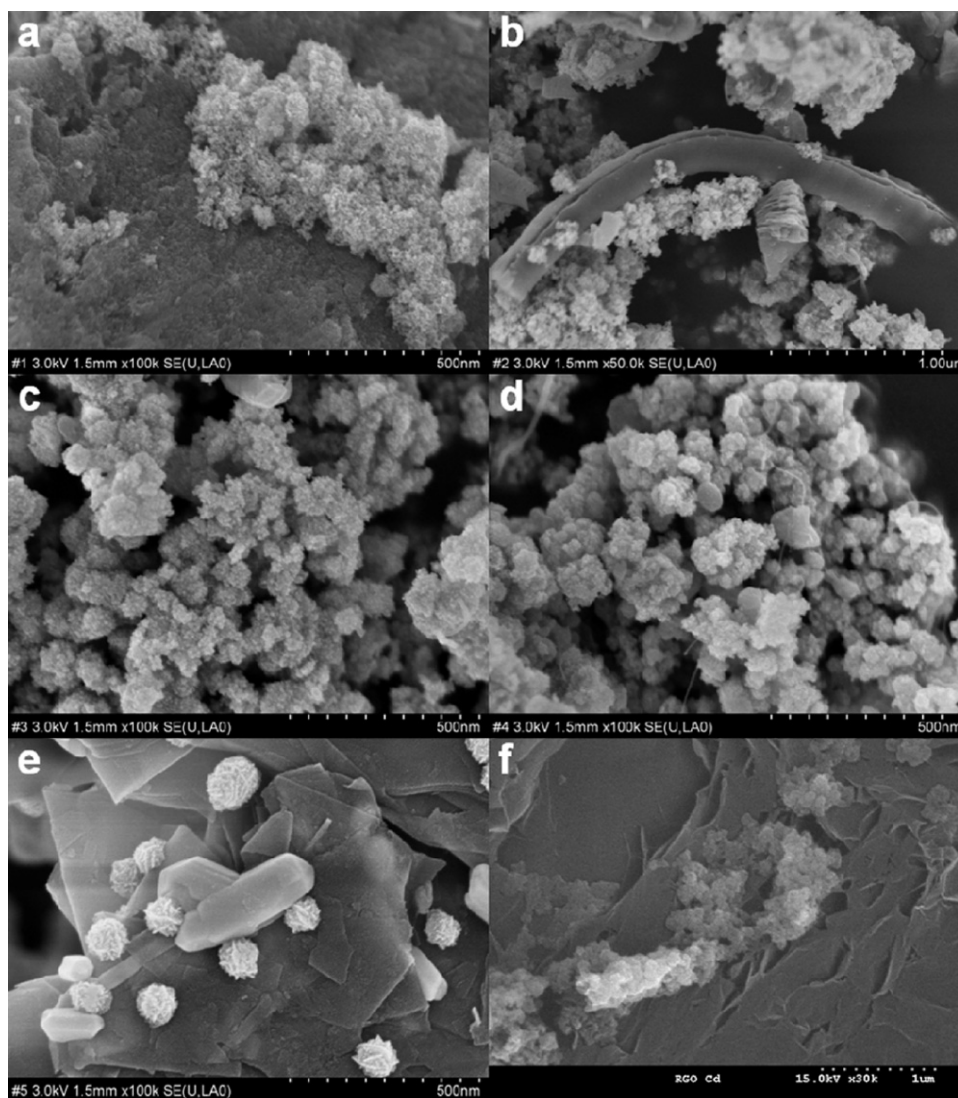
Fig. 2. SEM images of CdSe composites with acid-treated carbon materials: (a) activated carbon, (b) carbon nanofibers, (c) multi-walled carbon nanotubes, (d) single-walled carbon nanotubes, (e) graphites, and (f) reduced graphene oxides.
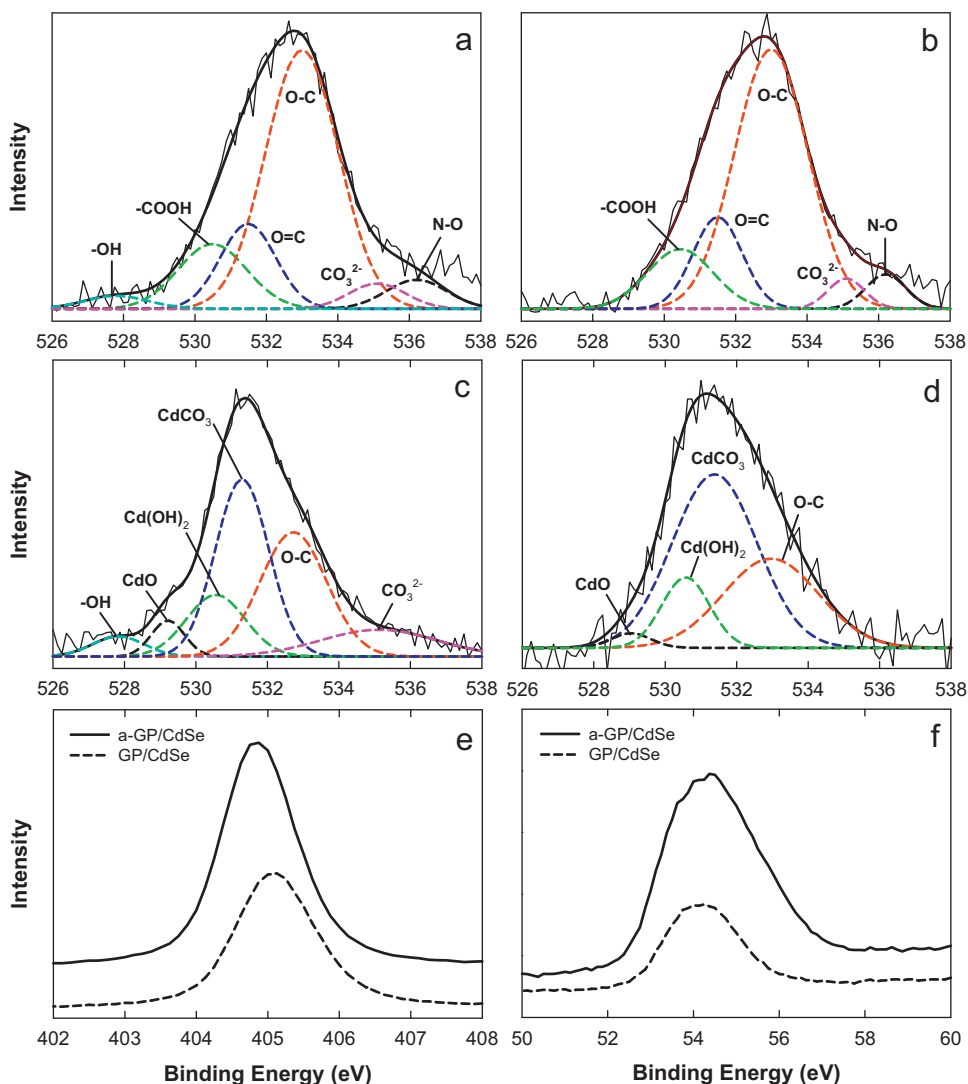
Fig. 3. XPS spectra of O 1s (a–d) for (a) virgin graphite (GP), (b) acid-treated graphite (a-GP), (c) GP/CdSe, (d) a-GP/CdSe samples. (e) and (f) also show the XPS spectra of Cd 3d and Se 3d, respectively, for GP/CdSe and a-GP/CdSe.

We have also examined the photoluminescence (PL) of the carbon/CdSe samples. The PL spectroscopy is a useful tool to study the recombination phenomena of photogenerated charge carriers at the surface of semiconductors [11,44]. As shown in Fig. 4, bare CdSe exhibited a strong PL band at around 590 nm corresponding to a primary particle size of around 4.5 nm [45]. When coupled to SWNT and GP, the main PL band was significantly reduced in intensity along with ca. 10 nm-shifts to short and long wavelength directions, respectively. Because of the size-dependent bandgap of CdSe, the position of its main PL band changes in the range between 550 nm (3.5 nm large) and 650 nm (7.0 nm large) [45]. However, such a change in the bandgaps of CdSe could not be found in the UV–vis absorption spectra of carbon/CdSe composites likely because of the strong background absorption of carbon materials (Fig. S2). GP/CdSe had an additional PL band at ~430 nm arising from graphite [46]. It should be pointed that the significant decreases in the PL band of CdSe by GP and SWNT indicates that the charge recombination is greatly inhibited by the carbon materials. Further, such decreases were even further advanced by employing a-GP and a-SWNT, suggesting that the recombination was more inhibited by the acid treatment as compared to the case of non-treated carbons (Fig. S3). This result, therefore, is
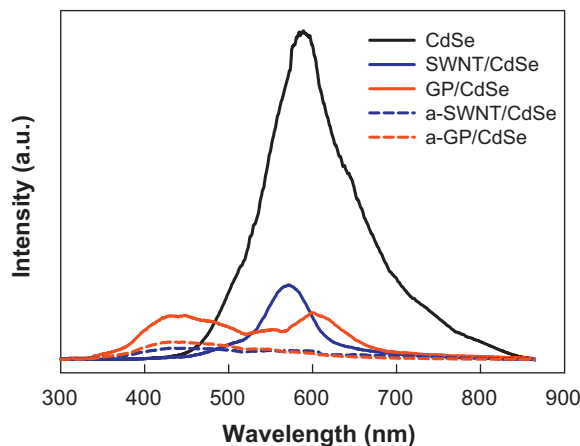

Fig. 4. Photoluminescence spectra of bare CdSe and carbon/CdSe composites.

qualitatively consistent with the findings that the H_2 productions of CdSe composites were much enhanced with acid-treated carbons.

3.2. Key factors of carbon materials catalyzing the hydrogen production

The major result of the aforementioned section is that the photocatalytic hydrogen production was significantly affected by the kind of carbon material and by the acid treatment of carbon material. Such phenomena could be studied in two aspects: CdSe effect and carbon effect.

3.2.1. CdSe effect

Although the same amount of CdSe was prepared on carbon materials, its actual amount loaded (or physically attached) on the carbon materials can be different. According to the SEM images of carbon/CdSe samples (Fig. 2), more CdSe particles appear to be formed on acid-treated carbon materials. Because the SEM images show only very limited local regions of entire sample surface, however, it is difficult to determine that acid-treated carbon materials have larger amounts of CdSe. If so, a straightforward way to quantify the amount of surface CdSe is most likely to estimate the amounts of Cd(II) adsorbed onto the carbon materials because the adsorbed Cd acts as a growing site of CdSe. It was found that when Cd(II) of 1×10^{-3} mol was mixed with carbon materials (0.06 g), approximately 74–85% of initial Cd(II) were adsorbed (Table 1). Acid treatment increased the amounts of Cd(II) adsorption, yet, marginally (max ~7%) [11]. It should be noted that adsorption of heavy metal cations including Cd(II) on carbon materials (natural carbons [47], activated carbon [48,49], CNT [50,51,52], etc.) is a complicated process with diverse operating mechanisms that highly depend on various factors [35,50] (e.g., surface oxygen complex content [50,51], pore texture [52], solution pH [48,49,52], ionic strength [47]). One of the primary factors in the adsorption of metal cation is the surface oxygen-containing groups of carbon materials, which generally increase the adsorption capacity for the metal cations [50,51]. In this study, the atomic percentages of oxygen-containing groups particularly able to bind Cd(II) (e.g., CO_3^{2-}) were similar with ~3–4 (e.g., between GP and a-GP samples. See Fig. 3). In addition, the contents of surface oxygen atom were similar with ca. 2% (GP vs. a-GP) and ~4–5% (GP/CdSe vs. a-GP/CdSe) (Table S1). All of these results suggest that the amounts of CdSe loaded on acid-treated carbon materials are larger than those on virgin carbon analogues, yet only marginally (~7%). However, the amounts of H_2 production were 3–6-fold enhanced by acid treatment, indicating that the effect of CdSe amount may be not significant.

3.2.2. Carbon effects

Although the carbon materials were used as platforms for CdSe, their unique physicochemical properties should contribute to the synergistic H_2 production. This study presumed the three properties of carbon materials (surface area, intensity ratio of disordered carbon and highly oriented pyrolytic graphite carbon in Raman spectra, and electrical conductivity) as key factors affecting the photocatalytic activity of CdSe for H_2 production.

3.2.3. Surface area

First of all, we examined if the surface area is the key factor in the H_2 production because the most prominent property of carbon materials is large surface area (Table 1). It was found that the surface areas of MWNT and GP were decreased by acid treatment, whereas those of the other carbons (AC, CNF, and SWNT) were increased. Yet the degrees of change in the surface areas appeared to be marginal (~10%). Indeed, the change of surface area by acid treatment has been reported to be small [53,54] and highly dependent on the kind of acid [53]. We have plotted the surface areas of carbon samples
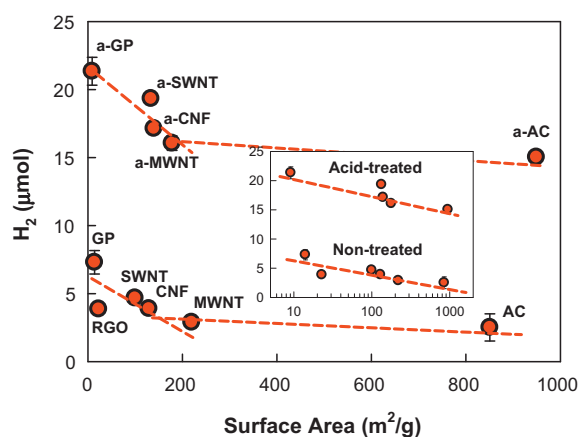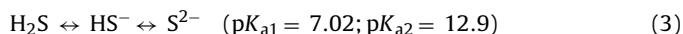

Fig. 5. Plot between surface areas of carbon materials and H_2 amounts produced from carbon/CdSe composites without and with acid treatment of carbon materials. Inset shows the plot of logarithmic surface areas vs. H_2 amounts.

vs. H_2 productions of the respective carbon/CdSe samples (Fig. 5). It is apparent that the H_2 amounts of carbon/CdSe decreased with the increasing surface area of carbon samples; MWNT/CdSe and AC/CdSe had similar activities despite the larger surface area of AC by a factor of 4. The negative effect of surface area of carbon samples is difficult to understand fully. A possible explanation is that carbon surface catalyzes the reduction of adsorbed polysulfides (S_{n+1}^{2-} and $(HS)_{n+1}^{-}$) that are produced from oxidation of sulfides (S^{2-}) by valence band holes (h_{vb}^{+}) (reactions (1)–(3)).

$$(n+1)S^{2-} + 2nh_{vb}^{+} \rightarrow S_{n+1}^{2-} \tag{1a}$$

$$S_{n+1}^{2-} + 2ne_{cb}^{-} \rightarrow (n+1)S^{2-} \tag{1b}$$

$$(n+1)HS^{-} + nh_{vb}^{+} \rightarrow (HS)_{n+1}^{-} \tag{2a}$$

$$(HS)_{n+1}^{-} + ne_{cb}^{-} \rightarrow (n+1)HS^{-} \tag{2b}$$

$$H_2S \leftrightarrow HS^{-} \leftrightarrow S^{2-} \quad (pK_{a1} = 7.02; pK_{a2} = 12.9) \tag{3}$$

Actually, carbon materials have been widely used as adsorbents for sulfides in industry, and the adsorption effect varies with many factors [35,55,56] (e.g., number of acidic groups, pH of surface, amounts of surface oxygen groups, etc.), all of which highly depend on the surface area. It is of note that despite the marginal change of surface area by acid treatment (~10%) the changes of H_2 amounts by the treatment were between ~300% and 570%. This indicates that the surface area may play a role of H_2 production but could not explain satisfactorily the enhanced H_2 production by acid treatment.

3.2.4. Graphitic property

The result that GP and SWNT induced the highest synergistic effect for H_2 production reveals that graphitic property of carbon materials, or inversely, degree of disordered carbon may be an important factor. To quantitatively compare this property among the carbon samples, Raman spectroscopic analyses for virgin and acid-treated carbon materials were performed (Fig. S4). Two distinct Raman bands were identically found for the carbon materials, which originate from disorder-induced amorphous carbon (D band) and highly oriented pyrolytic graphite (G band) [57,58]. The positions of each band were slightly different among the carbon materials due to inhomogeneous particle or tube sizes, varying defect density, and rough sample surface [59], yet they were similar with ~1280–1350 cm^{-1} (D band) and ~1590–1605 cm^{-1} (G band). The relative intensities of D band with respect to G band (I_D/I_G), therefore, are the indicator for the disordered carbon density (or degree of graphitic carbon in the case of I_G/I_D). It was
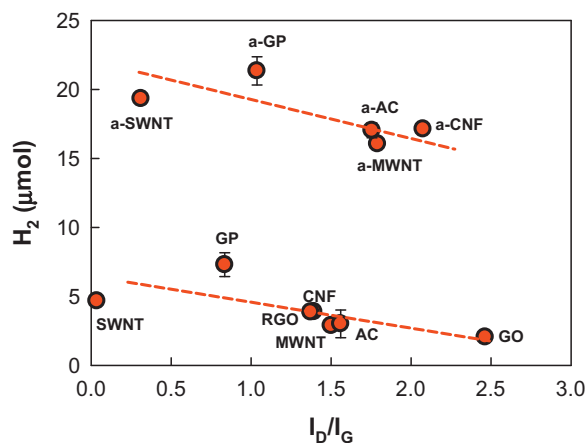
Fig. 6. Plot between I_D/I_G ratios of carbon materials and H_2 amounts produced from carbon/CdSe composites without and with acid treatment of carbon materials.
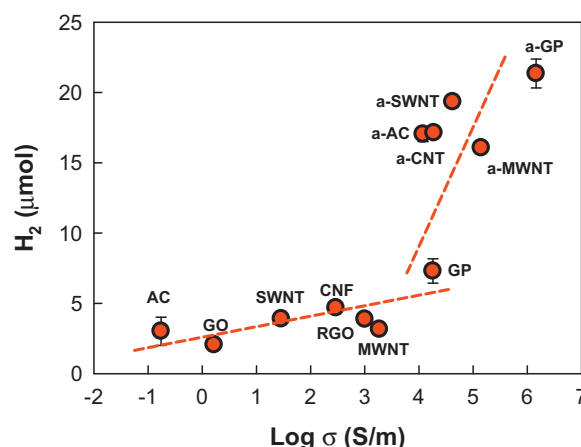

Fig. 7. Plot between electrical conductivities of carbon materials and H_2 amounts produced from carbon/CdSe composites without and with acid treatment of carbon materials.

found that SWNT and GP have the smallest I_D/I_G values while AC has the largest (Table 1). The I_D/I_G values of acid-treated carbon materials are greater than those of the respective virgin carbon materials because of oxidation by acid [59–62]. Fig. 6 shows the plots between the H_2 amounts and the I_D/I_G values. It is obvious that the H_2 amounts decrease with increasing the I_D/I_G values. This tendency is reasonable because as the I_D/I_G value increases the degree of graphitic carbon becomes less, and, thus, the catalytic effect of carbon materials may decrease. The same tendency was also found for the acid-treated carbons. Nevertheless, I_D/I_G value may not explain satisfactorily why the acid treatment significantly enhances the H_2 production.

3.2.5. Electrical conductivity

Finally, we considered the electrical conductivity (σ) the primary factor determining the overall H_2 production because for effective H_2 production the photogenerated electrons should be freely transported on carbon materials. It was found that GP and MWNT have around seven orders of magnitude greater conductivities than AC, CNF, and GO. Surprisingly, the acid treatment of carbon materials significantly increased the electrical conductivities of the respective virgin carbon materials by two orders of magnitude (e.g., MWNT, SWNT, and GP), probably due to removal of dangling carbons and unorganized carbon structure. Literature study indicates that the effects of acid treatment on the electrical conductivities (or resistivities) of carbon materials vary quite significantly. Derman et al. obtained a positive correlation for carbon pellets between electrical conductivity and (nitric) acid concentration [63], whereas the electrical conductivity of activated carbon-fiber cloths decreased by max. 32 times by treatment with mixed acid (nitric and sulfuric) [64]. Skakalova et al. showed that the electrical conductivity of SWNT is significantly increased by treating with $SOCl_2$, H_2SO_3, H_2SO_4, etc. (ionic acceptor doping-induced effect) [60]. These results therefore suggest that the acid treatment effects on the electrical conductivity of carbon materials are difficult to generalize. In this context, this study considered the electrical conductivities of carbon materials obtained through our own measurement. The plots between the H_2 amount vs. electrical conductivity ($\log \sigma$) are shown in Fig. 7. It is apparent that the H_2 amounts increase linearly with increasing $\log \sigma$ of carbon materials, and the slope becomes much steeper with acid-treated carbon materials (by approximately 10-fold). This indicates that the electrical conductivity is a critical factor in the H_2 production, explaining well the acid-treatment effect on the enhanced H_2 production. However it should be noted that the correlation for the H_2 amounts was obtained with $\log \sigma$, not with normal σ, suggesting

that the electrical conductivity effect is somewhat alleviated. The electrical conductivity is prerequisite for facile electron transfer from CdSe to neighboring carbon materials. Yet the H_2 production (i.e., proton reduction) needs additional elementary reactions including proton adsorption on carbon materials, coupling of two H atoms, and desorption of H_2 (reactions (4)–(7)), all of which are related to the catalytic property of carbon materials including surface area and I_D/I_G ratio as discussed above.

$$H^+(aq) \rightarrow H^+_{ads} \tag{4}$$

$$H^+_{ads} + e^-_{CdSe \rightarrow carbon} \rightarrow H_{ads} \tag{5}$$

$$H_{ads} + H_{ads} \rightarrow H_{2,ads} \tag{6}$$

$$H_{2,ads} \rightarrow H_2(g) \tag{7}$$

4. Conclusions

This study compared the photocatalytic H_2 production in visible light-irradiated carbon/CdSe composites with seven different carbon materials and attempted to find key factors for enhanced photocatalytic H_2 production. It was found that most carbon materials are beneficial in catalyzing H_2 production and that the catalytic effects were further increased by acid treatment of carbon materials. Systematic investigation on the relationship between the H_2 production and the bulk physicochemical properties of carbon materials revealed the following: (1) the surface area of carbon materials played a limited (even negative) role in the H_2 production; (2) as the degrees of disordered carbon (I_D/I_G ratios) were increased, the H_2 amounts decreased linearly; and (3) the H_2 amounts had a correlation with the logarithmic electrical conductivities of carbon materials. Further, acid treatment of carbon materials significantly enhanced the photocatalytic H_2 production of carbon/CdSe composites along with increases in the electrical conductivities of carbon materials. However, other properties of carbon materials (surface area, I_D/I_G ratios, Cd adsorption, etc.) were insignificantly changed by acid treatment. These results therefore strongly suggest that the electrical conductivity of carbon materials should be a primary factor in determining the overall photocatalytic H_2 production. High electrical conductivity appears to facilitate the photogenerated electron transfer from CdSe to neighboring carbon materials, leading to inhibition of charge pair recombination as evidenced by photoluminescence study (Scheme 1). Nevertheless, the linear fashion of H_2 amounts against logarithmic electrical conductivity further reveals that

other properties of carbon materials also are important in catalyzing H_2 production from water.

Acknowledgment

Appendix A. Supplementary data

Supplementary data associated with this article can be found, in the online version, at http://dx.doi.org/10.1016/j.apcatb.2012.06.018.

References

[1] C.A. Grimes, O.K. Varghese, S. Ranjan, Light, Water, Hydrogen, Springer, 2008.
[2] K. Maeda, K. Domen, The Journal of Physical Chemistry Letters 1 (2010) 2655–2661.
[3] B.D. James, G.N. Baum, J. Perez, K.N. Baum, Technoeconomic Analysis of Photoelectrochemical Hydrogen Production, DOE Contract Number: GS-10F-009J, December 2009.
[4] J. Greeley, T.F. Jaramillo, J. Bonde, I. Chorkendorff, J.K. Norskov, Nature Materials 5 (2006) 909–913.
[5] P. Serp, J.L. Figueiredo, Carbon Materials for Catalysis, Wiley, New Jersey, 2009.
[6] A.C. Dillon, Chemical Reviews 110 (2010) 6856–6872.
[7] Y.H. Ng, A. Iwase, A. Kudo, R. Amal, The Journal of Physical Chemistry Letters 1 (2010) 2607–2612.
[8] I. Willner, L. Sheeney-Haj-Khia, B. Basnar, Angewandte Chemie International Edition in English 44 (2005) 78–83.
[9] Y.H. Ng, I.V. Lightcap, K. Goodwin, M. Matsumura, P.V. Kamat, The Journal of Physical Chemistry Letters 1 (2010) 2222–2227.
[10] I. Robel, B.A. Bunker, P.V. Kamat, Advanced Materials 17 (2005) 2458–2463.
[11] Y.K. Kim, H. Park, Energy & Environmental Science 4 (2011) 685–694.
[12] L. Jia, D.-H. Wang, Y.-X. Huang, A.-W. Xu, H.-Q. Yu, Journal of Physical Chemistry C 115 (2011) 11466–11473.
[13] Q. Li, B. Guo, J. Yu, J. Ran, B. Zhang, H. Yan, J.R. Gong, Journal of the American Chemical Society 2011 (2011) 10878–10884.
[14] T. Torimoto, Y. Okawa, N. Takeda, H. Yoneyama, Journal of Photochemistry and Photobiology A 103 (1997) 153–157.
[15] S. Kim, S.K. Lim, Applied Catalysis B: Environmental 84 (2008) 16–20.
[16] R. Yuan, J. Zheng, R. Guan, Y. Zhao, Colloid Surface A 254 (2005) 131–136.
[17] A. Kongkanand, R.M. Dominguez, P.V. Kamat, Nano Letters 7 (2007) 676–680.
[18] K. Woan, G. Pyrgiotakis, W. Sigmund, Advanced Materials 21 (2009) 2233–2239.
[19] L. Sheeney-Haj-Khia, B. Basnar, I. Willner, Angewandte Chemie International Edition in English 44 (2005) 78–83.
[20] K.H. Ji, D.M. Jang, Y.J. Cho, Y. Myung, H.S. Kim, Y. Kim, J. Park, Journal of Physical Chemistry C 113 (2009) 19966–19972.
[21] A. Modestov, V. Glezer, I. Marjasin, O. Lev, Journal of Physical Chemistry B 101 (1997) 4623–4629.
[22] T.-F. Yeh, J.-M. Syu, C. Cheng, T.-H. Chagn, H. Teng, Advanced Functional Materials 20 (2010) 2255–2262.
[23] L.-W. Zhang, H.-B. Fu, Y.-F. Zhu, Advanced Functional Materials 18 (2008) 2180–2189.
[24] O. Akhavan, M. Abdolahad, A. Esfandiar, M. Mohatashamifar, Journal of Physical Chemistry C 114 (2010) 12955–12959.
[25] Y. Park, S.-H. Kang, W. Choi, Physical Chemistry Chemical Physics 13 (2011) 9425–9431.
[26] H. Zhang, X.J. Lv, Y.M. Li, Y. Wang, J.H. Li, ACS Nano 4 (2010) 380–386.
[27] I.V. Lightcap, T.H. Kosel, P.V. Kamat, Nano Letters 10 (2010) 577–583.
[28] W. Fan, Q. Lai, Q. Zhang, Y. Wang, Journal of Physical Chemistry C 115 (2011) 10694–10701.
[29] N.J. Bell, H.N. Yun, A.J. Du, H. Coster, S.C. Smith, R. Amal, Journal of Physical Chemistry C 115 (2011) 6004–6009.
[30] Y.H. Zhang, Z.R. Tang, X.Z. Fu, Y.J. Xu, ACS Nano 4 (2010) 7303–7314.
[31] A. Kongkanand, P.V. Kamat, ACS Nano 1 (2007) 13–21.
[32] H. Kim, G. Moon, D. Monllor-Satoca, Y. Park, W. Choi, Journal of Physical Chemistry C (2011), http://dx.doi.org/10.1021/jp209035e.
[33] Y. Wang, R. Shi, J. Lin, Y. Zhu, Applied Catalysis B: Environmental 100 (2010) 179–183.
[34] T. Xu, L. Zhang, H. Cheng, Y. Zhu, Applied Catalysis B: Environmental 101 (2011) 382–387.
[35] E.J. Bottani, J.D. Tascon (Eds.), Adsorption by Carbons, Elsevier, New York, 2008.
[36] W.S. Hummers, R.E. Offeman, Journal of the American Chemical Society 80 (1958) 1339.
[37] Y.-L. Lee, C.-F. Chi, S.-Y. Liau, Chemistry of Materials 22 (2010) 922–927.
[38] N. Lakshminarasimhan, E. Bae, W. Choi, Journal of Physical Chemistry C 111 (2007) 15244–15250.
[39] N. Lakshminarasimhan, W. Kim, W. Choi, Journal of Physical Chemistry C 112 (2008) 20451–20457.
[40] S.K. Choi, S. Kim, S.K. Lim, H. Park, Journal of Physical Chemistry C 114 (2010) 16475–16480.
[41] http://srdata.nist.gov/xps/Default.aspx. (accessed November 2011).
[42] R. Nyholm, N. Martensson, Solid State Communications 40 (1981) 311–314.
[43] J.S. Hammond, S.W. Gaarenstroom, N. Winograd, Analytical Chemistry 47 (1975) 2193–2199.
[44] H. Park, Y.K. Kim, W. Choi, Journal of Physical Chemistry C 115 (2011) 6141–6148.
[45] A. Javier, C.S. Yun, J. Sorena, G.F. Strouse, Journal of Physical Chemistry B 107 (2003) 435–442.
[46] S.-S. Chang, Materials Science and Engineering B 106 (2004) 56–62.
[47] J. Hanzlik, J. Jehlicka, O. Sebek, Z. Weishauptova, V. Machovic, Water Research 38 (2004) 2178–2184.
[48] K. Periasamy, C. Namasivayam, Industrial and Engineering Chemistry Research 33 (1994) 317–320.
[49] P. Marzal, A. Seco, C. Gabaldon, Journal of Chemical Technology and Biotechnology 66 (1996) 279–285.
[50] X. Ren, C. Chen, M. Nagatsu, X. Wang, Chemical Engineering Journal 170 (2011) 395–410.
[51] H.-H. Cho, K. Wepasnick, B.A. Smith, F.K. Bangash, D.H. Fairbrother, W.P. Ball, Langmuir 26 (2010) 967–981.
[52] Y.-H. Li, S. Wang, Z. Luan, J. Ding, C. Xu, D. Wu, Carbon 41 (2003) 1057–1062.
[53] C. Moreno-Castilla, M.A. Ferro-Garcia, J.P. Joly, I. Bautista-Toledo, F. Carrasco-Marin, J. Rivera-Utrilla, Langmuir 11 (1995) 4386–4392.
[54] J.S. Noh, J.A. Schwarz, Carbon 28 (1990) 675–682.
[55] A. Bagreev, T.J. Bandosz, Industrial and Engineering Chemistry Research 41 (2002) 672–679.
[56] F. Adib, A. Bagreev, T.J. Bandosz, Environmental Science and Technology 34 (2000) 686–692.
[57] M.S. Dresselhaus, G. Dresselhaus, R. Saito, A. Jorio, Physics Reports: Review Section of Physics Letters 409 (2005) 47–99.
[58] A. Cuesta, P. Dhamelincourt, J. Laureyns, A. Martinez-Alonso, J.M.D. Tascon, Carbon 32 (1994) 1523–1532.
[59] S. Osswald, M. Havel, Y. Gogotsi, Journal of Raman Spectroscopy 38 (2007) 728–736.
[60] V. Skakalova, A.B. Kaiser, U. Dettlaff-Weglikowska, K. Hrncarikova, S. Roth, Journal of Physical Chemistry B 109 (2005) 7174–7181.
[61] L. Shao, G. Tobias, C.G. Salzmann, B. Ballesteros, S.Y. Hong, A. Crossely, B.G. Davis, M.L.H. Green, Chemical Communications (2007) 5090–5092.
[62] H.-Z. Geng, K.K. Kim, K.P. So, Y.S. Lee, Y. Chang, Y.H. Lee, Journal of the American Chemical Society 129 (2007) 7758–7759.
[63] M. Derman, R. Omar, S. Zakaria, I.R. Mustapa, M. Talib, N. Alias, R. Jaafar, Journal of Materials Science 37 (2002) 3329–3335.
[64] Z. Hashisho, M.J. Rood, S. Barot, J. Bernhard, Carbon 47 (2009) 1814–1823.